Journal of Beijing Institute of Technology, 2025, Vol. 34, No. 6

Adaptive Neural Control for Hypersonic Vehicle Based on Barrier Lyapunov Function

Hewei Zhao✉, Chengcheng Wang, Jing Sun
(Naval Aviation University, Yantai 264001, Shandong, China)

Abstract: In this paper, an adaptive neural backstepping control method based on barrier Lyapunov function is proposed for hypersonic vehicle considering full state constraints. The longitudinal dynamic of hypersonic vehicle can be divided into two subsystems, i.e., altitude subsystem and velocity subsystem and the controllers are designed with backstepping method, respectively. In the designing process, the radial basis function neural networks are used to approximate the unknown nonlinear functions of longitudinal dynamic, therefore, the accuracy requirement of hypersonic vehicle model is largely reduced. In order to handle the explosion of complexity issues occurring in the backstepping method, a tracking differentiator is introduced to calculate the differential of virtual control law. The barrier Lyapunov function is constructed to overcome the full system dynamic state constraints and an auxiliary system is designed for overcome the input state saturation issue. The stability is carried out based on Lyapunov theory, and the signals of closed-loop system established are uniformly ultimately bounded. The simulation results show that the controller designed for hypersonic vehicle can guarantee the good tracking performance.

Keywords: hypersonic vehicle; barrier Lyapunov function; radial basis function neural network; tracking differentiator

1 Introduction

Hypersonic vehicle is a near space flight vehicle with the speed over five mach. A growing number of researchers have focus on the study of hypersonic vehicle which represents the ability to use near space. However, there are many challenges of hypersonic vehicle research field needed to be overcome. In recent years, a large number of research results have emerged. Normally, the matched uncertainties and mismatched uncertainties exist in the nonlinear system of hypersonic vehicle. The backstepping control method can be used to solve the matched and mismatched uncertainties issues. Backstepping control method is a nonlinear control strategy widely used in controller design for strict feedback system of flight vehicle [1–7]. However, the differentiation calculation of virtual controller is so difficult to carry out, i.e., explosion of complexity issue. In many papers, the filtering method is proposed to handle the explosion problem [8–12], the differentiation of virtual controller can be replaced by filtering signal, but so far, there is no systematic methodology to select the control gains and the time constants of the filters. Moreover, the estimating errors will be introduced into the state feedback process and the state tracking accuracy is reduced, because of the tracking errors are defined with the signals occurred from filters. In lots of papers, an tracking differentiator methodology is used to estimate some unknown nonlinearity, the sophistication of tracking differentiator method is that the stability of overall system is easy to be proved,

Manuscript received Apr. 1, 2025; revised Nov. 30, 2025; accepted Dec. 1, 2025. The associate editor coordinating the review of this manuscript was Dr. Junjie Wu. This work was supported by the National Natural Science Foundation of China (No. 61903374).
✉ Corresponding author. Email: lf815fe@sina.cn
DOI: 10.15918/j.jbit1004-0579.2025.018

and adaptability of the controller for the control gain changes can be raised. In the controller design process, the unmodeled dynamic issue of hypersonic vehicle system is mostly ignored in many papers, obviously some shortcomings exist in this control design strategy. For example, in the backstepping design process, the neural network algorithm is introduced to approximate the unknown unmodeled nonlinear system dynamic [13–17], and normally, the partial parameters of neural network are updated with adaptive laws. With this estimation method, the accuracy requirement of flight vehicle dynamic system model is largely reduced.

Furthermore, for the hypersonic vehicle system dynamic, the system input-output states are constraints needed to be overcome. This is one of the main challenges of control system design for hypersonic vehicle. Input saturation caused by the constraints of the magnitude, if these constraints are neglected in the control design, rate of actuators can degrade the performance of the control system or even lead to instability [18]. In some papers [19, 20], the influence of input constraints can be properly avoided with the auxiliary system design. However, these strategies cannot be applied to output constrained problems. In recent years, a barrier Lyapunov function strategy is used to handle output constraints in the process of controller design [21–26]. However, input constraints are not taken into consideration in those control schemes. Certainly, the full state constraints issues have not been solved in aforementioned papers.

Different from previous work, in this paper, the full state constraints issue is considered based on barrier Lyapunov function, and the input saturation is overcome with an auxiliary system. All states of hypersonic vehicle system can be constrained within a certain range, which is accord with the actual engineering requirements. The explosion of complexity raised from backstepping method is handled with a tracking differentiator. In the progress of controller design, the ideal virtual controller is used to define the state tracking error introduced into the feedback process, and the tracking accuracy can be guaranteed. Considering the model perturbation and parameter uncertainty, the adaptive radial basis function neural network is used to approximate the unknown unmodeled nonlinear dynamic of hypersonic vehicle. In this paper, problem formulation of hypersonic vehicle dynamic model is described in Section 2. The adaptive radial basis function neural network backstepping controller design based on barrier Lyapunov function will be proposed in Section 3, the explosion problem arising from backstepping method will be avoided by the tracking differentiator, moreover, the input saturation issue will be handled with an auxiliary system. The stability analysis for velocity subsystem and altitude subsystem will be described in Section 4, respectively. And in Section 5, to demonstrate its usefulness, simulation will be carried out to verify the effectiveness of controller proposed. Finally, conclusion and future works are discussed in Section 6.

2 Problem Formulation

The longitudinal dynamic model of hypersonic vehicle in this study is given in [27]. The detail form can be described as follow. There are five rigid-body state variables involved in the model, i.e., V, h, γ, α, Q, while the four flexible state variables are not considered in this study. Moreover, the control inputs are δ_e, i.e., elevator deflection and Φ, i.e., fuel equivalence ratio.

$$\dot{V} = \frac{1}{m}(T\cos\alpha - D) - g\sin(\theta - \alpha) \tag{1}$$

$$\dot{h} = V sin(\theta - \alpha) \tag{2}$$

$$\dot{\alpha} = \frac{1}{mV}(-T\sin\alpha - L) + Q + \frac{g}{V}\cos(\theta - \alpha) \tag{3}$$

$$\dot{\theta} = Q \tag{4}$$

$$I_{yy}\dot{Q} = M \tag{5}$$

where V is the velocity, h is the altitude, γ is the flight path angle, α is the attack angle, Q is the pitch rate, m is the mass of aircraft, g is the acceleration due to gravity, θ is the angle of pitch, moreover, T, D, L, M represent the thrust, drag, lift-force, and pitching moment, respectively. And I_{yy} is the moment of inertia about pitch axis.

The related expressions are described as follow.

$$L = \frac{1}{2}\rho V^2 S C_L \tag{6}$$

$$D = \frac{1}{2}\rho V^2 S C_D \tag{7}$$

$$M = z_T T + \frac{1}{2}\rho V^2 S\bar{c}[C_{M,\alpha} + C_{M,\delta_e}] \tag{8}$$

$$T = C_T^{\alpha^3}\alpha^3 + C_T^{\alpha^2}\alpha^2 + C_T^{\alpha}\alpha + C_T^0 \tag{9}$$

where S is aircraft reference area, $\bar{c}$ is Average aerodynamic chord length, $\rho = \rho_0 \exp[-(h-h_0)/h_s]$, $C_L = C_L^{\alpha}\alpha + C_L^0$, $C_D = C_D^{\alpha^2}\alpha^2 + C_D^{\alpha}\alpha + C_D^0$, $C_{M,\alpha} = C_{M,\alpha}^{\alpha^2}\alpha^2 + C_{M,\alpha}^{\alpha}\alpha + C_{M,\alpha}^0, C_{M,\delta_e} = c_e\delta_e, C_T^{\alpha^3} = \beta_1\Phi + \beta_2$, $C_T^{\alpha^2} = \beta_3\Phi + \beta_4$, $C_T^{\alpha} = \beta_5\Phi + \beta_6$, $C_T^0 = \beta_7\Phi + \beta_8$.

The detail information of parameter values are described in [27]. It is easy to see that $\theta = \alpha + \gamma$, the Eqs. (1)–(5) can be expressed as

$$\dot{V} = \frac{1}{m}(T\cos\alpha - D) - g\sin\gamma \tag{10}$$

$$\dot{h} = V sin\gamma \tag{11}$$

$$\dot{\alpha} = \frac{1}{mV}(-T\sin\alpha - L) + Q + \frac{g}{V}\cos\gamma \tag{12}$$

$$\dot{\theta} = Q \tag{13}$$

$$I_{yy}\dot{Q} = M \tag{14}$$

The Eq. (10) is the velocity subsystem, The Eqs. (11)–(14) are altitude subsystem. Although the longitudinal dynamics of the aircraft are divided into two subsystems, but they are not completely decoupled.

3 Controllers Design

The dynamics of model (10)–(14) can be decomposed into altitude subsystem and velocity subsystem since the velocity is mainly related to thrust force and the altitude is mainly affected by elevator deflection. Firstly, the controller of velocity subsystem is designed as follows.

3.1 Controller Design for Velocity Subsystem

According to the dynamic (10), we can obtain

$$\dot{V} = f_V + \Phi \tag{15}$$

where $f_V = \frac{1}{m}(T\cos\alpha - D) - g\sin\gamma - \Phi$ is an unknown nonlinear function.

For the velocity subsystem, the RBF neural network is applied to approximate the unknown nonlinear function f_V in dynamic (10).

Lemma 1 Radial basis function neural network (RBFNN) can be used to approximate an unknown nonlinear function as follows.

$$f = \boldsymbol{W}^{*\mathrm{T}}\phi(\boldsymbol{x}) + \varepsilon \tag{16}$$

where f is a unknown nonlinear function, $\boldsymbol{W}^*$ is the optimal weight vector, $\phi(\boldsymbol{x}) = [\phi_1(\boldsymbol{x}), \phi_2(\boldsymbol{x}), \cdots, \phi_l(\boldsymbol{x})]$ is the radial basis function, $\boldsymbol{x}$ is the input vector of NN, and ε is the construction error of neural network with the supreme ε_{1m}. Moreover, the radial basis function $\phi_i(\boldsymbol{x})$ can be described as

$$\phi_i(\boldsymbol{x}) = \exp(-(\boldsymbol{x} - c_i)^{\mathrm{T}}(\boldsymbol{x} - c_i)/b_i^2) \tag{17}$$

According to Lemma 1, it is easy to obtain

$$f_V = \boldsymbol{W}_V^{*\mathrm{T}}\phi_V(\boldsymbol{x}_V) + \varepsilon_V \tag{18}$$

where ε_V denotes approximate error with the supreme ε_{Vm}, i.e., $|\varepsilon_V| \leqslant \varepsilon_{Vm}$.

Lemma 2 In this paper, the barrier Lyapunov function (BLF) is used to complete the controller design [19], BLF can be described as

$$L = \frac{1}{2}\log\left(\frac{k_b^2}{k_b^2 - z^2}\right) \tag{19}$$

where $\log(\cdot)$ is the natural logarithm function, k_b denotes the smooth performance function, normally, the follow conditions can be satisfied [21]:

(a) k_b is a positive monotone decreasing function.

(b) $\lim\limits_{t\to\infty} k_b = k_b^{\infty}$.

The performance function can be defined as $k_b = (k_b^0 - k_b^{\infty})e^{-lt} + k_b^{\infty}$. In this paper, k_b is selected as a positive constant and seen as the constraint on state error z, i.e., $|z| < k_b$. For any positive constant k_b, the following inequality [22] holds for all z in the interval $|z| < k_b$, and the inequality will be used in the stability analysis of control system.

$$\log\left(\frac{k_b^2}{k_b^2 - z^2}\right) < \frac{z^2}{k_b^2 - z^2} \tag{20}$$

Define the tracking error of velocity as

$$z_V = V - V_d - \vartheta_V \tag{21}$$

where V_d is the reference velocity, and ϑ_V is the signal generated from auxiliary system constructed as follows

$$\dot{\vartheta}_V + k_{aV}\vartheta_V = \tilde{\Phi} \tag{22}$$

ϑ_V can be used to deal with input signal saturation issue. In Eq. (22), error signal $\tilde{\Phi} = \Phi - \Phi_d$, where Φ is the control input of velocity subsystem with considering saturation issue, and Φ_d is the control input signal needed to be designed without considering saturation issue. k_{aV} is a positive design parameter.

The time derivative of z_V can be described as

$$\dot{z}_V = \dot{V} - \dot{V}_d - \dot{\vartheta}_V \tag{23}$$

Invoking (15) and (22) yields

$$\dot{z}_V = f_V - \dot{V}_d + \Phi_d + k_{aV}\vartheta_V \tag{24}$$

Considering (18), we can obtain

$$\dot{z}_V = \boldsymbol{W}_V^{*\mathrm{T}}\phi_V(x_V) + \varepsilon_V - \dot{V}_d + \Phi_d + k_{aV}\vartheta_V \tag{25}$$

The velocity controller can be designed as

$$\begin{aligned}\Phi_d = &- k_V z_V - \hat{\boldsymbol{W}}_V^{\mathrm{T}}\phi_V - k_{aV}\vartheta_V + \dot{V}_d - \\ &\hat{\varepsilon}_V \tanh\left(\frac{z_V}{\delta_V(k_{bV}^2 - z_V^2)}\right)\end{aligned} \tag{26}$$

where k_V is a positive design parameter, $\hat{\boldsymbol{W}}_V$ is the estimation of $\boldsymbol{W}_V^*$, $\hat{\varepsilon}_V$ is the estimation of ε_{Vm}, and $\delta_V > 0$ is design parameter. The estimation errors can be defined as $\tilde{\boldsymbol{W}}_V = \boldsymbol{W}_V^* - \hat{\boldsymbol{W}}_V$, $\tilde{\varepsilon}_V = \varepsilon_{Vm} - \hat{\varepsilon}_V$.

By substituting (26) into (25), it yields

$$\begin{aligned}\dot{z}_V = &- k_V z_V + \tilde{\boldsymbol{W}}_V^{\mathrm{T}}\phi_V + \varepsilon_V - \\ &\varepsilon_{Vm}\tanh\left(\frac{z_V}{\delta_V(k_{bV}^2 - z_V^2)}\right) + \\ &\tilde{\varepsilon}_V \tanh\left(\frac{z_V}{\delta_V(k_{bV}^2 - z_V^2)}\right)\end{aligned} \tag{27}$$

A barrier Lyapunov function can be constructed in a form of

$$L_V = \frac{1}{2}\log\left(\frac{k_{bV}^2}{k_{bV}^2 - z_V^2}\right) + \frac{1}{2}\tilde{\boldsymbol{W}}_V^{\mathrm{T}}\Gamma_V^{-1}\tilde{\boldsymbol{W}}_V + \frac{1}{2\varpi_V}\tilde{\varepsilon}_V^2 \tag{28}$$

where Γ_V, ϖ_V are positive design parameters.

It is easy to obtain the differentiation of (28) as follows

$$\dot{L}_V = \frac{z_V\dot{z}_V}{k_{bV}^2 - z_V^2} - \dot{\hat{\boldsymbol{W}}}_V^{\mathrm{T}}\Gamma_V^{-1}\tilde{\boldsymbol{W}}_V - \frac{1}{\varpi_V}\dot{\hat{\varepsilon}}_V\tilde{\varepsilon}_V \tag{29}$$

Invoking (26) and (29) yields

$$\begin{aligned}\dot{L}_V = &- \frac{k_V z_V^2}{k_{bV}^2 - z_V^2} + \frac{z_V\tilde{W}_V^T\phi_V}{k_{bV}^2 - z_V^2} + \\ &\frac{z_V}{k_{bV}^2 - z_V^2}\left(\varepsilon_V - \varepsilon_{Vm}\tanh\left(\frac{z_V}{\delta_V(k_{bV}^2 - z_V^2)}\right) + \right. \\ &\left.\tilde{\varepsilon}_V\tanh\left(\frac{z_V}{\delta_V(k_{bV}^2 - z_V^2)}\right)\right) - \dot{\hat{\boldsymbol{W}}}_V^T\Gamma_V^{-1}\tilde{\boldsymbol{W}}_V - \\ &\frac{1}{\varpi_V}\dot{\hat{\varepsilon}}_V\tilde{\varepsilon}_V\end{aligned} \tag{30}$$

The updating laws for $\hat{\boldsymbol{W}}_V$, $\hat{\varepsilon}_V$, respectively, can be designed as follows:

$$\dot{\hat{W}}_V = \Gamma_V\left(\frac{z_V}{k_{bV}^2 - z_V^2}\phi_V - \lambda_V\hat{\boldsymbol{W}}_V\right) \tag{31}$$

$$\dot{\hat{\varepsilon}}_V = \varpi_V\left[\frac{z_V}{k_{bV}^2 - z_V^2}\tanh\left(\frac{z_V}{\delta_V(k_{bV}^2 - z_V^2)}\right) - \sigma_V\hat{\varepsilon}_V\right] \tag{32}$$

where λ_V, σ_V are the positive design parameters.

Substituting the updating algorithm (31), (32) into (30), it yields

$$\begin{aligned}\dot{L}_V = &- \frac{k_V z_V^2}{k_{bV}^2 - z_V^2} + \lambda_V\hat{\boldsymbol{W}}_V^{\mathrm{T}}\tilde{\boldsymbol{W}}_V + \sigma_V\hat{\varepsilon}_V\tilde{\varepsilon}_V + \\ &\frac{z_V}{k_{bV}^2 - z_V^2}\left[\varepsilon_V - \varepsilon_{Vm}\tanh\left(\frac{z_V}{\delta_V(k_{bV}^2 - z_V^2)}\right)\right]\end{aligned} \tag{33}$$

3.2 Controller Design for Altitude Subsystem

Based on the timescale conclusion from [14], it is obvious that the velocity can be considered as slow dynamic compared with the state variables of altitude subsystem, therefore the velocity will be treated as constant during the controller design for altitude subsystem. For the altitude subsystem, the flight path command is designed as [15]

$$\gamma_d = \frac{-k_h(h-h_r) - k_i\int(h-h_r)\mathrm{d}t + \dot{h}_r}{V} \tag{34}$$

where k_h, k_i are positive constants, h_r is the reference altitude, if the flight path angle can follow γ_d, then the altitude tracking error $\tilde{h} = h - h_r$ can be regulated to zero exponentially. According to [8], we have

$$\dot{\gamma}_d \approx \frac{-k_h(V\sin\gamma - \dot{h}_r) - k_i\tilde{h} + \ddot{h}_r}{V} \tag{35}$$

Assumption 1 In (12), it is easy to know that the term $T\sin\alpha$ is generally much smaller than L, which can be neglected. This assumption has been used in lots of preliminary papers, which is reasonable for controller design.

Define $x_1 = \gamma$, $x_2 = \theta$, $x_3 = Q$, and $\boldsymbol{X} = [x_1, x_2, x_3]^{\mathrm{T}}$, based on A1, the altitude subsystem (12)–(14) can be written in a form of

$$\dot{x}_1 = g_1 x_2 + f_1(x_1) \tag{36}$$

$$\dot{x}_2 = x_3 \tag{37}$$

$$\dot{x}_3 = f_3(X) + u \tag{38}$$

$$y = x_1 \tag{39}$$

where $g_1 = \dfrac{\rho V S}{2m}C_L^{\alpha}$, $f_1 = -\dfrac{\rho V S}{2m}C_L^{\alpha}x_1 - \dfrac{g}{V}\cos x_1 + \dfrac{\rho V S}{2m}C_L^0$, $g_3 = \dfrac{1}{2I_{yy}}\rho V^2 S\bar{c}c_e$, $f_3 = \dfrac{z_T T}{I_{yy}} + \dfrac{1}{2I_{yy}}\rho V^2 S\bar{c}(C_{M,\alpha} + C_{M,\delta_e}) - u$.

In (36)–(39), $\boldsymbol{X} = [x_1, x_2, x_3]^{\mathrm{T}} \in R^3$, $u \in R$, and $y \in R$ are the state, input and output of the altitude subsystem, respectively. It is obvious that g_1, g_3 are known constants, with out of generality, some assumptions are essential in the sequel.

Assumption 2 The reference output y_d is bounded and smooth.

Assumption 3 The state vector $\boldsymbol{X}$ is measurable.

Assumption 4 The nonlinear functions f_1, f_3 are unknown and bounded.

In the assumptions, it is easy to know that y_d is the reference output designed according to the engineering practice, moreover the states can be measured and bounded are proved in many previous research, thus, the assumptions are reasonable.

In this section, the backstepping method will be used to design attitude controller, and the tracking differentiators are developed to deal with the explosion of complexity occurred from backstepping method.

Step 1 For the dynamic (36), define the tracking errors of flight path angle as

$$z_1 = \gamma - \gamma_d = x_1 - x_{1d} \tag{40}$$

The differentiation of z_1 is obtained as follows:

$$\dot{z}_1 = \dot{x}_1 - \dot{x}_{1d} = g_1 x_2 + f_1 - \dot{x}_{1d} \tag{41}$$

Likewise, the unknown nonlinear function f_1 can be estimated with RBF NN such that

$$f_1 = \boldsymbol{W}_1^{*\mathrm{T}}\phi_1 + \varepsilon_1 \tag{42}$$

where $\boldsymbol{W}_1^*$, ε_1 denote the optimal weight vector and estimation error with the supreme ε_{1m}, respectively.

Substituting (42) into (41), it yields

$$\dot{z}_1 = g_1 x_2 + \boldsymbol{W}_1^{*\mathrm{T}}\phi_1 + \varepsilon_1 - \dot{x}_{1d} \tag{43}$$

Define the other error as

$$z_2 = x_2 - x_{2v} \tag{44}$$

where x_{2v} is the virtual controller, for the error dynamic (43), we can obtain

$$\dot{z}_1 = g_1 z_2 + g_1 x_{2v} + \boldsymbol{W}_1^{*\mathrm{T}}\phi_1 + \varepsilon_1 - \dot{x}_{1d} \tag{45}$$

The virtual controller can be designed as

$$x_{2v} = g_1^{-1}\Big(-k_1 z_1 - \hat{\boldsymbol{W}}_1^{\mathrm{T}}\phi_1 + \dot{x}_{1d} - \hat{\varepsilon}_1\tanh\Big(\frac{z_1}{\delta_1(k_{b1}^2 - z_1^2)}\Big)\Big) \tag{46}$$

where k_1 is the positive design parameter, $\hat{\boldsymbol{W}}_1$, $\hat{\varepsilon}_1$

are the estimations of $\boldsymbol{W}_1^*$, ε_{1m}, respectively. The errors can be defined as $\tilde{\boldsymbol{W}}_1 = \boldsymbol{W}_1^* - \hat{\boldsymbol{W}}_1$ and $\tilde{\varepsilon}_1 = \varepsilon_{1m} - \hat{\varepsilon}_1$,$\hat{\varepsilon}_1 \tanh\left(\dfrac{z_1}{\delta_1(k_{b1}^2 - z_1^2)}\right)$ is a robust compensator.

Substituting (46) into (45), it yields

$$\dot{z}_1 = -k_1 z_1 + g_1 z_2 + \tilde{\boldsymbol{W}}_1^{\mathrm{T}}\phi_1 + \varepsilon_1 - \varepsilon_{1m}\tanh\left(\frac{z_1}{\delta_1(k_{b1}^2 - z_1^2)}\right) + \tilde{\varepsilon}_1 \tanh\left(\frac{z_1}{\delta_1(k_{b1}^2 - z_1^2)}\right) \tag{47}$$

The barrier Lyapunov function can be constructed as

$$L_1 = \frac{1}{2}\log\left(\frac{k_{b1}^2}{k_{b1}^2 - z_1^2}\right) + \frac{1}{2}\tilde{\boldsymbol{W}}_1^{\mathrm{T}}\Gamma_1^{-1}\tilde{\boldsymbol{W}}_1 + \frac{1}{2\varpi_1}\tilde{\varepsilon}_1^2 \tag{48}$$

where Γ_1, ϖ_1 are positive design parameters. $k_{b1}$is the constraint of z_1, i.e., $|z_1| < k_{b1}$. The direct differentiation of L_1 can be calculated as

$$\dot{L}_1 = \frac{z_1\dot{z}_1}{k_{b1}^2 - z_1^2} + \dot{\tilde{\boldsymbol{W}}}_1^{\mathrm{T}}\Gamma_1^{-1}\tilde{\boldsymbol{W}}_1 + \frac{1}{\varpi_1}\tilde{\varepsilon}_1\dot{\tilde{\varepsilon}}_1 = \frac{z_1\dot{z}_1}{k_{b1}^2 - z_1^2} - \dot{\hat{\boldsymbol{W}}}_1^{\mathrm{T}}\Gamma_1^{-1}\tilde{\boldsymbol{W}}_1 - \frac{1}{\varpi_1}\tilde{\varepsilon}_1\dot{\hat{\varepsilon}}_1 \tag{49}$$

Invoking (47) and (49), it yields

$$\dot{L}_1 = -\frac{k_1 z_1^2}{k_{b1}^2 - z_1^2} + \frac{g_1 z_1 z_2}{k_{b1}^2 - z_1^2} + \frac{z_1\tilde{\boldsymbol{W}}_1^{\mathrm{T}}\phi_1}{k_{b1}^2 - z_1^2} + \frac{z_1\varepsilon_1}{k_{b1}^2 - z_1^2} - \frac{z_1\varepsilon_{1m}}{k_{b1}^2 - z_1^2}\tanh\left(\frac{z_1}{\delta_1(k_{b1}^2 - z_1^2)}\right) + \frac{z_1\tilde{\varepsilon}_1}{k_{b1}^2 - z_1^2}\tanh\left(\frac{z_1}{\delta_1(k_{b1}^2 - z_1^2)}\right) - \dot{\hat{\boldsymbol{W}}}_1^{\mathrm{T}}\Gamma_1^{-1}\tilde{\boldsymbol{W}}_1 - \frac{1}{\varpi_1}\tilde{\varepsilon}_1\dot{\hat{\varepsilon}}_1 \tag{50}$$

The adaptive updating laws can be designed as follows.

$$\dot{\hat{\boldsymbol{W}}}_1 = \Gamma_1\left(\frac{z_1}{k_{b1}^2 - z_1^2}\phi_1 - \lambda_1\hat{\boldsymbol{W}}_1\right) \tag{51}$$

$$\dot{\hat{\varepsilon}}_1 = \varpi_1\left[\frac{z_1}{k_{b1}^2 - z_1^2}\tanh\left(\frac{z_1}{\delta_1(k_{b1}^2 - z_1^2)}\right) - \sigma_1\hat{\varepsilon}_1\right] \tag{52}$$

Considering the above adaptive laws, we can obtain

$$\dot{L}_1 = -\frac{k_1 z_1^2}{k_{b1}^2 - z_1^2} + \frac{g_1 z_1 z_2}{k_{b1}^2 - z_1^2} + \frac{z_1\varepsilon_1}{k_{b1}^2 - z_1^2} - \frac{z_1\varepsilon_{1m}}{k_{b1}^2 - z_1^2}\tanh\left(\frac{z_1}{\delta_1(k_{b1}^2 - z_1^2)}\right) + \lambda_1\hat{\boldsymbol{W}}_1^{\mathrm{T}}\tilde{\boldsymbol{W}}_1 + \sigma_1\hat{\varepsilon}_1\tilde{\varepsilon}_1 \tag{53}$$

Step 2 The differentiation of tracking error z_2 can be calculated as

$$\dot{z}_2 = \dot{x}_2 - \dot{x}_{2v} = x_3 - \dot{x}_{2v} \tag{54}$$

Obviously, the calculation of the differentiation term $\dot{x}_{2v}$ is so difficult and in order to avoid the tedious analytical computations involved in the controller design process, the tracking differentiator is used to deal with the explosion of complexity question. $\dot{x}_{2v}$ can be estimated with a tracking differentiator described in [28].

Lemma 3 Considering the following system in a form of

$$\begin{cases} \dot{d}_1 = d_2 \\ \dot{d}_2 = \zeta^2 F(d_1 - \vartheta(t), d_2/\zeta) \end{cases} \tag{55}$$

where d_1, d_2 are the states of tracking differentiator system, $\zeta > 0$ is the design parameter, and $F(\psi_1, \psi_2) = v(\psi_1) + v(\psi_2)$, $v(\cdot)$ is designed as [28]

$$v(\psi) = \begin{cases} -\kappa\dfrac{\ln(1 + |\psi|)}{|\psi|}\psi, & \psi \neq 0 \\ 0, & \psi = 0 \end{cases} \tag{56}$$

where $\kappa > 0$ is the design parameter. The conclusion has been proved in [28], i.e., $|d_1 - \vartheta|$ and $\left|d_2 - \dot{\vartheta}\right|$ are bounded in a limited time scale. Thus, the following tracking differentiator is used to estimate the first-order differential of x_{2v}.

$$\begin{cases} \dot{d}_{11} = d_{12} \\ \dot{d}_{12} = \zeta_1^2 F(d_{11} - x_{2v}, d_{12}/\zeta_1) \end{cases} \tag{57}$$

According to Lemma 3, we know that $\dot{x}_{2v}^d = d_{12}$, moreover, the following inequality holds

$$|\dot{x}_{2v} - \dot{x}_{2v}^d| \leqslant \varepsilon_1^d \tag{58}$$

where $\varepsilon_1^d > 0$ is the estimate error which can guarantee the tracking accuracy.

Define $z_3 = x_3 - x_{3v} - \vartheta_3$, where x_{3v} is the virtual controller, ϑ_3 is the signal generated from an auxiliary system constructed as follows

$$\dot{\vartheta}_3 + k_{a3}\vartheta_3 = \tilde{u} \tag{59}$$

In (59), error signal $\tilde{u} = u - u_d$, where u is the control input of altitude subsystem with considering saturation issue, and u_d is the control

input signal needed to be designed without considering saturation issue. k_{a3} is a positive design parameter.

Thus, we can obtain

$$\dot{z}_2 = z_3 + x_{3v} + \vartheta_3 - \dot{x}_{2v} \tag{60}$$

The virtual controller x_{3v} can be designed as

$$x_{3v} = -k_2 z_2 - \frac{g_1 z_1 (k_{b2}^2 - z_2^2)}{k_{b1}^2 - z_1^2} + \dot{x}_{2v}^d - \vartheta_3 - \frac{z_2}{2(k_{b2}^2 - z_2^2)} \tag{61}$$

Substituting (61) into (60), it yields

$$\dot{z}_2 = z_3 - k_2 z_2 - \frac{g_1 z_1 (k_{b2}^2 - z_2^2)}{k_{b1}^2 - z_1^2} + \dot{x}_{2v}^d - \dot{x}_{2v} - \frac{z_2}{2(k_{b2}^2 - z_2^2)} \tag{62}$$

The barrier Lyapunov function can be constructed as

$$L_2 = \frac{1}{2} \log \left(\frac{k_{b2}^2}{k_{b2}^2 - z_2^2} \right) \tag{63}$$

where k_{b2} is the constraint of z_2, i.e., $|z_2| < k_{b2}$.

The direct differential of (62) is calculated as

$$\dot{L}_2 = \frac{z_2 \dot{z}_2}{k_{b2}^2 - z_2^2} \tag{64}$$

By invoking (62) and (64), we obtain

$$\begin{aligned} \dot{L}_2 = & -\frac{k_2 z_2^2}{k_{b2}^2 - z_2^2} + \frac{z_2 z_3}{k_{b2}^2 - z_2^2} - \frac{g_1 z_1 z_2}{k_{b1}^2 - z_1^2} + \\ & \frac{z_2}{k_{b2}^2 - z_2^2} (\dot{x}_{2v}^d - \dot{x}_{2v}) - \frac{z_2^2}{2(k_{b2}^2 - z_2^2)^2} \end{aligned} \tag{65}$$

Step 3 For the dynamic (38), f_3 is considered as an unknown nonlinear function, as done previously, an RBF NN can be used to approximate f_3. The differential of z_3 can be described as

$$\begin{aligned} \dot{z}_3 = & \dot{x}_3 - \dot{x}_{3v} - \dot{\vartheta}_3 = f_3 + u - \dot{x}_{3v} - \dot{\vartheta}_3 = \\ & \boldsymbol{W}_3^{*\mathrm{T}} \phi_3 + \varepsilon_3 - \dot{x}_{3v} + k_{a3} \vartheta_3 + u_d \end{aligned} \tag{66}$$

where $\boldsymbol{W}_3^*$, ε_3 denote the optimal weight vector and the approximation error with the supreme ε_{1m}, respectively.

Likewise, $\dot{x}_{3v}$ can be estimated with a tracking differentiator in a form of

$$\begin{cases} \dot{d}_{31} = d_{32} \\ \dot{d}_{32} = \zeta_3^2 F(d_{31} - x_{3v}, d_{32}/\zeta_3) \end{cases} \tag{67}$$

According to Lemma 3, we know that $\dot{x}_{3v}^d = d_{32}$, moreover, the following inequality holds

$$|\dot{x}_{3v} - \dot{x}_{3v}^d| \leqslant \varepsilon_3^d \tag{68}$$

where $\varepsilon_3^d > 0$ is the estimate error.

Obviously, the overall control law u in (66) can be designed as

$$\begin{aligned} u_d = & -k_3 z_3 - \frac{z_2 (k_{b3}^2 - z_3^2)}{k_{b2}^2 - z_2^2} - \hat{\boldsymbol{W}}_3^{\mathrm{T}} \phi_3 - k_{a3} \vartheta_3 - \\ & \hat{\varepsilon}_3 \tanh \left(\frac{k_{b3}^2}{\delta_3 (k_{b3}^2 - z_3^2)} \right) + \dot{x}_{3v}^d - \frac{z_3}{2(k_{b3}^2 - z_3^2)} \end{aligned} \tag{69}$$

Substituting (69) into (66), it yields

$$\begin{aligned} \dot{z}_3 = & -k_3 z_3 - \frac{z_2 (k_{b3}^2 - z_3^2)}{k_{b2}^2 - z_2^2} + \tilde{\boldsymbol{W}}_3^{\mathrm{T}} \phi_3 + \varepsilon_3 - \\ & \varepsilon_{3m} \tanh \left(\frac{k_{b3}^2}{\delta_3 (k_{b3}^2 - z_3^2)} \right) + \\ & \tilde{\varepsilon}_3 \tanh \left(\frac{k_{b3}^2}{\delta_3 (k_{b3}^2 - z_3^2)} \right) + \\ & \dot{x}_{3v}^d - \dot{x}_{3v} - \frac{z_3}{2(k_{b3}^2 - z_3^2)} \end{aligned} \tag{70}$$

A barrier Lyapunov function can be given as

$$L_3 = \frac{1}{2} \log \left(\frac{k_{b3}^2}{k_{b3}^2 - z_3^2} \right) + \frac{1}{2} \tilde{\boldsymbol{W}}_3^{\mathrm{T}} \Gamma_3^{-1} \tilde{\boldsymbol{W}}_3 + \frac{1}{2\varpi_3} \tilde{\varepsilon}_3^2 \tag{71}$$

where Γ_3, ϖ_3 are positive design parameters. k_{b3} is the constraint of z_3, i.e., $|z_3| < k_{b3}$. The direct differential of (71) is given by

$$\dot{L}_3 = \frac{z_3 \dot{z}_3}{k_{b3}^2 - z_3^2} + \dot{\tilde{\boldsymbol{W}}}_3^{\mathrm{T}} \Gamma_3^{-1} \tilde{\boldsymbol{W}}_3 + \frac{1}{\varpi_3} \tilde{\varepsilon}_3 \dot{\tilde{\varepsilon}}_3 \tag{72}$$

Substituting (70) into (72), it is rewritten as

$$\begin{aligned} \dot{L}_3 = & -\frac{k_3 z_3^2}{k_{b3}^2 - z_3^2} - \frac{z_2 z_3}{k_{b2}^2 - z_2^2} + \frac{z_3 \tilde{\boldsymbol{W}}_3^{\mathrm{T}} \phi_3}{k_{b3}^2 - z_3^2} + \\ & \frac{z_3}{k_{b3}^2 - z_3^2} \left(\varepsilon_3 - \varepsilon_{3m} \tanh \left(\frac{k_{b3}^2}{\delta_3 (k_{b3}^2 - z_3^2)} \right) \right) + \\ & \frac{z_3 \tilde{\varepsilon}_3}{k_{b3}^2 - z_3^2} \tanh \left(\frac{k_{b3}^2}{\delta_3 (k_{b3}^2 - z_3^2)} \right) + \\ & \frac{z_3}{k_{b3}^2 - z_3^2} (\dot{x}_{3v}^d - \dot{x}_{3v}) + \dot{\tilde{\boldsymbol{W}}}_3^{\mathrm{T}} \Gamma_3^{-1} \tilde{\boldsymbol{W}}_3 + \\ & \frac{1}{\varpi_3} \tilde{\varepsilon}_3 \dot{\tilde{\varepsilon}}_3 - \frac{z_3^2}{2(k_{b3}^2 - z_3^2)^2} \end{aligned} \tag{73}$$

The adaptive updating laws can be designed

as

$$\dot{\hat{\boldsymbol{W}}}_3 = \Gamma_3 \left(\frac{z_3}{k_{b3}^2 - z_3^2} \phi_3 - \lambda_3 \hat{\boldsymbol{W}}_3 \right) \tag{74}$$

$$\dot{\hat{\varepsilon}}_3 = \varpi_3 \left[\frac{z_3}{k_{b3}^2 - z_3^2} \tanh\left(\frac{z_3}{\delta_3 (k_{b3}^2 - z_3^2)} \right) - \sigma_3 \hat{\varepsilon}_3 \right] \tag{75}$$

Considering the adaptive laws, (73) is rewritten as

$$\begin{aligned} \dot{L}_3 = & - \frac{k_3 z_3^2}{k_{b3}^2 - z_3^2} - \frac{z_2 z_3}{k_{b2}^2 - z_2^2} + \\ & \frac{z_3}{k_{b3}^2 - z_3^2} \left(\varepsilon_3 - \varepsilon_{3m} \tanh\left(\frac{k_{b3}^2}{\delta_3 (k_{b3}^2 - z_3^2)} \right) \right) + \\ & \frac{z_3}{k_{b3}^2 - z_3^2} (\dot{x}_{3v}^d - \dot{x}_{3v}) + \lambda_3 \hat{\boldsymbol{W}}_3^{\mathrm{T}} \tilde{\boldsymbol{W}}_3 + \\ & \sigma_3 \hat{\varepsilon}_3 \tilde{\varepsilon}_3 - \frac{z_3^2}{2(k_{b3}^2 - z_3^2)^2} \end{aligned} \tag{76}$$

4 Stability Analysis

The overall control system is consisting of two control subsystems, i.e., velocity control subsystem and attitude control subsystem, the stability analysis are carried out respectively.

4.1 Stability Analysis for Velocity Subsystem

Based on the results from [17], the following inequality holds

$$0 \leqslant |\eta| - \eta \tanh\left(\frac{\eta}{\delta} \right) \leqslant c_\eta \delta, \eta \in R \tag{77}$$

where c_η is selected as 0.2785, δ is a positive constant.

Considering the inequality (77), (33) can be described as

$$\dot{L}_V \leqslant - \frac{k_V z_V^2}{k_{bV}^2 - z_V^2} + \lambda_V \hat{\boldsymbol{W}}_V^{\mathrm{T}} \tilde{\boldsymbol{W}}_V + \sigma_V \hat{\varepsilon}_V \tilde{\varepsilon}_V + c_\eta \varepsilon_{Vm} \delta_V \tag{78}$$

For easy reference, we quote the following inequalities here:

$$\hat{\boldsymbol{W}}_V^{\mathrm{T}} \tilde{\boldsymbol{W}}_V \leqslant \frac{1}{2} \|\boldsymbol{W}_V^*\|^2 - \frac{1}{2} \left\| \tilde{\boldsymbol{W}}_V \right\|^2 \tag{79}$$

$$\hat{\varepsilon}_V \tilde{\varepsilon}_V \leqslant \frac{1}{2} \varepsilon_{Vm}^2 - \frac{1}{2} \tilde{\varepsilon}_V^2 \tag{80}$$

The inequalities can be found in references [8], the reasonable has been proved.

Invoking (78), (79) and (80), we obtain

$$\begin{aligned} \dot{L}_V \leqslant & - \frac{k_V z_V^2}{k_{bV}^2 - z_V^2} - \frac{1}{2} \lambda_V \|\tilde{\boldsymbol{W}}_V\|^2 - \frac{1}{2} \sigma_V \tilde{\varepsilon}_V^2 + \\ & \frac{1}{2} \lambda_V \|\boldsymbol{W}_V^*\|^2 + \frac{1}{2} \sigma_V \varepsilon_{Vm}^2 + c_\eta \varepsilon_{Vm} \delta_V \end{aligned} \tag{81}$$

Considering the inequality (20) in Lemma 2, (81) is given by

$$\begin{aligned} \dot{L}_V \leqslant & - k_V \log\left(\frac{k_{bV}^2}{k_{bV}^2 - z_V^2} \right) - \frac{1}{2} \lambda_V \|\tilde{\boldsymbol{W}}_V\|^2 - \frac{1}{2} \sigma_V \tilde{\varepsilon}_V^2 + \\ & \frac{1}{2} \lambda_V \|\boldsymbol{W}_V^*\|^2 + \frac{1}{2} \sigma_V \varepsilon_{Vm}^2 + c_\eta \varepsilon_{Vm} \delta_V \end{aligned} \tag{82}$$

Consider (33), we have

$$\dot{L}_V \leqslant -\zeta_V L_V + C_V \tag{83}$$

with $\zeta_V = \min\left[2k_V, \frac{\lambda_V}{\lambda_{\max}(\Gamma_V^{-1})}, \sigma_V \varpi_V \right]$, $C_V = \frac{1}{2} \lambda_V \|\boldsymbol{W}_V^*\|^2 + \frac{1}{2} \sigma_V \varepsilon_{Vm}^2 + c_\eta \varepsilon_{Vm} \delta_V$.

Multiplying (83) by $e^{\zeta_V t}$, we have

$$\frac{\mathrm{d}}{\mathrm{d}t} (L_V e^{\zeta_V t}) \leqslant C_V e^{\zeta_V t} \tag{84}$$

Integrating above inequality, we obtain

$$L_V \leqslant \left(L_V(0) - \frac{C_V}{\zeta_V} \right) e^{-\zeta_V t} + \frac{C_V}{\zeta_V} \tag{85}$$

Therefore, we have

$$\frac{1}{2} \log\left(\frac{k_{bV}^2}{k_{bV}^2 - z_V^2} \right) \leqslant L_V(0) + \frac{C_V}{\zeta_V} \tag{86}$$

$$|z_V| \leqslant k_{bV} \sqrt{(1 - \mathrm{e}^{-2(L_V(0) + C_V/\zeta_V)})} < k_{bV} \tag{87}$$

Likewise, we obtain

$$\left| \tilde{\boldsymbol{W}}_V \right| \leqslant \sqrt{\frac{2}{\lambda_{\min}(\Gamma_V^{-1})} (L_V(0) + C_V/\zeta_V)} \tag{88}$$

$$|\tilde{\varepsilon}_V| \leqslant \sqrt{2(L_V(0) + C_V/\zeta_V)} \tag{89}$$

According to the analysis above, the conclusion can be obtained as follows.

Theorem 1 Considering the velocity subsystem consisting of the plant (15), controller (26), and the adaptive updating laws (31), (32), all the signals in the closed-loop system are uniformly ultimately bounded with the control parameters selected reasonably. Furthermore, the velocity tracking error z_V, RBF NN parameters

estimation errors $\tilde{\boldsymbol{W}}_V$, $\tilde{\varepsilon}_V$ can converge to the compact set described as (88), (89).

4.2 Stability Analysis for Altitude Subsystem

Choose the Lyapunov function in a form of

$$L = L_1 + L_2 + L_3 \tag{90}$$

where L_1, L_2, L_3 have been defined as (48), (63), (71), therefore we know$L > 0$. Furthermore, the differential of (90) can be described as

$$\begin{aligned}\dot{L} =&\dot{L}_1 + \dot{L}_2 + \dot{L}_3 = \\ &-\frac{k_1 z_1^2}{k_{b1}^2 - z_1^2} - \frac{k_2 z_2^2}{k_{b2}^2 - z_2^2} - \frac{k_3 z_3^2}{k_{b3}^2 - z_3^2} + \\ &\frac{z_1 \varepsilon_1}{k_{b1}^2 - z_1^2} - \frac{z_1 \varepsilon_{1m}}{k_{b1}^2 - z_1^2} \tanh\left(\frac{z_1}{\delta_1 (k_{b1}^2 - z_1^2)}\right) + \\ &\frac{z_3}{k_{b3}^2 - z_3^2}\left(\varepsilon_3 - \varepsilon_{3m} \tanh\left(\frac{k_{b3}^2}{\delta_3 (k_{b3}^2 - z_3^2)}\right)\right) + \\ &\lambda_1 \hat{\boldsymbol{W}}_1^{\mathrm{T}} \tilde{\boldsymbol{W}}_1 + \sigma_1 \hat{\varepsilon}_1 \tilde{\varepsilon}_1 + \lambda_3 \hat{\boldsymbol{W}}_3^{\mathrm{T}} \tilde{\boldsymbol{W}}_3 + \sigma_3 \hat{\varepsilon}_3 \tilde{\varepsilon}_3 + \\ &\frac{z_2}{k_{b2}^2 - z_2^2}(\dot{x}_{2v}^d - \dot{x}_{2v}) + \frac{z_3}{k_{b3}^2 - z_3^2}(\dot{x}_{3v}^d - \dot{x}_{3v}) - \\ &\frac{z_2^2}{2(k_{b2}^2 - z_2^2)^2} - \frac{z_3^2}{2(k_{b3}^2 - z_3^2)^2}\end{aligned} \tag{91}$$

Based on the inequality (77), we can obtain

$$\begin{aligned}\dot{L} \leqslant &-\frac{k_1 z_1^2}{k_{b1}^2 - z_1^2} - \frac{k_2 z_2^2}{k_{b2}^2 - z_2^2} - \frac{k_3 z_3^2}{k_{b3}^2 - z_3^2} + \varepsilon_{1m} c_\eta \delta_1 + \\ &\varepsilon_{3m} c_\eta \delta_3 + \lambda_1 \hat{\boldsymbol{W}}_1^{\mathrm{T}} \tilde{\boldsymbol{W}}_1 + \sigma_1 \hat{\varepsilon}_1 \tilde{\varepsilon}_1 + \lambda_3 \hat{\boldsymbol{W}}_3^{\mathrm{T}} \tilde{\boldsymbol{W}}_3 + \\ &\sigma_3 \hat{\varepsilon}_3 \tilde{\varepsilon}_3 + \frac{z_2}{k_{b2}^2 - z_2^2}(\dot{x}_{2v}^d - \dot{x}_{2v}) + \\ &\frac{z_3}{k_{b3}^2 - z_3^2}(\dot{x}_{3v}^d - \dot{x}_{3v}) - \frac{z_2^2}{2(k_{b2}^2 - z_2^2)^2} - \\ &\frac{z_3^2}{2(k_{b3}^2 - z_3^2)^2}\end{aligned}$$

[−1*pt*]

(92)

Consider the following inequalities

$$\hat{\boldsymbol{W}}_1^{\mathrm{T}} \tilde{\boldsymbol{W}}_1 \leqslant \frac{1}{2}\|\boldsymbol{W}_1^*\|^2 - \frac{1}{2}\|\tilde{\boldsymbol{W}}_1\|^2 \tag{93}$$

$$\hat{\varepsilon}_1 \tilde{\varepsilon}_1 \leqslant \frac{1}{2}\varepsilon_{1m}^2 - \frac{1}{2}\tilde{\varepsilon}_1^2 \tag{94}$$

$$\hat{\boldsymbol{W}}_3^{\mathrm{T}} \tilde{\boldsymbol{W}}_3 \leqslant \frac{1}{2}\|\boldsymbol{W}_3^*\|^2 - \frac{1}{2}\|\tilde{\boldsymbol{W}}_3\|^2 \tag{95}$$

$$\hat{\varepsilon}_3 \tilde{\varepsilon}_3 \leqslant \frac{1}{2}\varepsilon_{3m}^2 - \frac{1}{2}\tilde{\varepsilon}_3^2 \tag{96}$$

The inequalities have been proved and used in Previous works.

Invoking (92) and (93)–(96), we have

$$\begin{aligned}\dot{L} \leqslant &-\frac{k_1 z_1^2}{k_{b1}^2 - z_1^2} - \frac{k_2 z_2^2}{k_{b2}^2 - z_2^2} - \frac{k_3 z_3^2}{k_{b3}^2 - z_3^2} - \\ &\frac{1}{2}\lambda_1 \|\tilde{\boldsymbol{W}}_1\|^2 - \frac{1}{2}\lambda_3 \|\tilde{\boldsymbol{W}}_3\|^2 - \frac{1}{2}\sigma_1 \tilde{\varepsilon}_1^2 - \frac{1}{2}\sigma_3 \tilde{\varepsilon}_3^2 + \\ &\varepsilon_{1m} c_\eta \delta_1 + \varepsilon_{3m} c_\eta \delta_3 + \frac{1}{2}\lambda_1 \|\boldsymbol{W}_1^*\|^2 + \\ &\frac{1}{2}\lambda_3 \|\boldsymbol{W}_3^*\|^2 + \frac{1}{2}\sigma_1 \varepsilon_{1m}^2 + \frac{1}{2}\sigma_3 \varepsilon_{3m}^2 - \\ &\frac{z_2}{k_{b2}^2 - z_2^2}(\dot{x}_{2v} - \dot{x}_{2v}^d) - \frac{z_3}{k_{b3}^2 - z_3^2}(\dot{x}_{3v} - \dot{x}_{3v}^d) - \\ &\frac{z_2^2}{2(k_{b2}^2 - z_2^2)^2} - \frac{z_3^2}{2(k_{b3}^2 - z_3^2)^2}\end{aligned} \tag{97}$$

Consider the following inequalities

$$-\frac{z_2}{k_{b2}^2 - z_2^2}(\dot{x}_{2v} - \dot{x}_{2v}^d) \leqslant \frac{1}{2}\frac{z_2^2}{(k_{b2}^2 - z_2^2)^2} + \frac{1}{2}(\varepsilon_1^d)^2 \tag{98}$$

$$-\frac{z_3}{k_{b3}^2 - z_3^2}(\dot{x}_{3v} - \dot{x}_{3v}^d) \leqslant \frac{1}{2}\frac{z_3^2}{(k_{b3}^2 - z_3^2)^2} + \frac{1}{2}(\varepsilon_3^d)^2 \tag{99}$$

Therefore we have

$$\begin{aligned}\dot{L} \leqslant &-\frac{k_1 z_1^2}{k_{b1}^2 - z_1^2} - \frac{k_2 z_2^2}{k_{b2}^2 - z_2^2} - \frac{k_3 z_3^2}{k_{b3}^2 - z_3^2} - \\ &\frac{1}{2}\lambda_1 \|\tilde{\boldsymbol{W}}_1\|^2 - \frac{1}{2}\lambda_3 \|\tilde{\boldsymbol{W}}_3\|^2 - \frac{1}{2}\sigma_1 \tilde{\varepsilon}_1^2 - \frac{1}{2}\sigma_3 \tilde{\varepsilon}_3^2 + \\ &\varepsilon_{1m} c_\eta \delta_1 + \varepsilon_{3m} c_\eta \delta_3 + \frac{1}{2}\lambda_1 \|\boldsymbol{W}_1^*\|^2 + \\ &\frac{1}{2}\lambda_3 \|\boldsymbol{W}_3^*\|^2 + \frac{1}{2}\sigma_1 \varepsilon_{1m}^2 + \frac{1}{2}\sigma_3 \varepsilon_{3m}^2 + \\ &\frac{1}{2}(\varepsilon_1^d)^2 + \frac{1}{2}(\varepsilon_3^d)^2\end{aligned} \tag{100}$$

Consider the inequality (20), (100) can be rewritten as

$$\begin{aligned}\dot{L} \leqslant &-k_1 \log\left(\frac{k_{b1}^2}{k_{b1}^2 - z_1^2}\right) - k_2 \log\left(\frac{k_{b2}^2}{k_{b2}^2 - z_2^2}\right) - \\ &k_3 \log\left(\frac{k_{b3}^2}{k_{b3}^2 - z_3^2}\right) - \frac{1}{2}\lambda_1 \|\tilde{\boldsymbol{W}}_1\|^2 - \frac{1}{2}\lambda_3 \|\tilde{\boldsymbol{W}}_3\|^2 - \\ &\frac{1}{2}\sigma_1 \tilde{\varepsilon}_1^2 - \frac{1}{2}\sigma_3 \tilde{\varepsilon}_3^2 + \varepsilon_{1m} c_\eta \delta_1 + \varepsilon_{3m} c_\eta \delta_3 + \\ &\frac{1}{2}\lambda_1 \|\boldsymbol{W}_1^*\|^2 + \frac{1}{2}\lambda_3 \|\boldsymbol{W}_3^*\|^2 + \frac{1}{2}\sigma_1 \varepsilon_{1m}^2 + \\ &\frac{1}{2}\sigma_3 \varepsilon_{3m}^2 + \frac{1}{2}(\varepsilon_1^d)^2 + \frac{1}{2}(\varepsilon_3^d)^2\end{aligned} \tag{101}$$

Thus we have

$$\dot{L} \leqslant -\sum_{i=1}^{3} \zeta_i L_i + C \tag{102}$$

with

$$\zeta_1 = \min\left[2k_1, \frac{\lambda_1}{\lambda_{\max}(\Gamma_1^{-1})}, \sigma_1\varpi_1\right]$$

$$\zeta_2 = 2k_2$$

$$\zeta_3 = \min[2k_3, \frac{\lambda_3}{\lambda_{\max}(\Gamma_3^{-1})}, \sigma_3\varpi_3]$$

$$C = \varepsilon_{1m}c_\eta\delta_1 + \varepsilon_{3m}c_\eta\delta_3 + \frac{1}{2}\lambda_1\|\boldsymbol{W}_1^*\|^2 + \frac{1}{2}\lambda_3\|\boldsymbol{W}_3^*\|^2 + \frac{1}{2}\sigma_1\varepsilon_{1m}^2 + \frac{1}{2}\sigma_3\varepsilon_{3m}^2 + \frac{1}{2}(\varepsilon_1^d)^2 + \frac{1}{2}(\varepsilon_3^d)^2.$$

Furthermore, we can obtain

$$\dot{L} \leqslant -\zeta L + C \tag{103}$$

where $\zeta = \min[\zeta_1, \zeta_2, \zeta_3]$. It is easy to know that C is a bounded constant.

Based on (103), we have

$$L \leqslant (L(0) - \frac{C}{\zeta})\mathrm{e}^{-\zeta t} + \frac{C}{\zeta} \tag{104}$$

Likewise, we have

$$|z_1| \leqslant k_{b1}\sqrt{(1 - \mathrm{e}^{-2(L(0)+C/\zeta)})} < k_{b1} \tag{105}$$

$$|z_2| \leqslant k_{b2}\sqrt{(1 - \mathrm{e}^{-2(L(0)+C/\zeta)})} < k_{b2} \tag{106}$$

$$|z_3| \leqslant k_{b3}\sqrt{(1 - \mathrm{e}^{-2(L(0)+C/\zeta)})} < k_{b3} \tag{107}$$

$$\left|\tilde{\boldsymbol{W}}_1\right| \leqslant \sqrt{\frac{2}{\lambda_{\min}(\Gamma_1^{-1})}(L(0) + C/\zeta)} \tag{108}$$

$$|\tilde{\varepsilon}_1| \leqslant \sqrt{2(L(0) + C/\zeta)} \tag{109}$$

$$\left|\tilde{\boldsymbol{W}}_2\right| \leqslant \sqrt{\frac{2}{\lambda_{\min}(\Gamma_2^{-1})}(L(0) + C/\zeta)} \tag{110}$$

$$|\tilde{\varepsilon}_2| \leqslant \sqrt{2(L(0) + C/\zeta)} \tag{111}$$

Theorem 2 Consider the closed-loop control system consisting of the plant (15), virtual controllers (46), (61) and the actual controller (69), and the NN adaptive updating laws (51), (22), (74), (75). If the control gain and tuning parameters can be selected reasonably, all the signals in the closed-loop system are uniformly ultimately bounded. Besides, tracking errors can converge uniformly to the following set described as (105)–(111).

5 Simulation

In this section, the simulation will be carried out for proving the effectiveness of control strategies, The control gains are selected as $k_1 = 2, k_2 = 8$, $k_3 = 1.2$, the auxiliary system parameters are designed as $k_{a3} = 10$, $k_{aV} = 15$, the state constraints are designed as $k_{bV} = 5, k_{b1} = 0.09$, $k_{b2} = 0.5$, $k_{b3} = 0.8$. The differentiator parameters are selected as $\kappa_1 = 0.5$, $\zeta_1 = 0.3$, $\kappa_2 = 0.6$, $\zeta_1 = 0.2$. Moreover, the updating laws parameters are selected as $\Gamma_V = 0.5$, $\lambda_V = 0.9$, $\varpi_V = 1.5$, $\sigma_V = 0.3$, $\Gamma_1 = 0.65$, $\lambda_1 = 0.75$, $\varpi_1 = 8$, $\sigma_1 = 0.2$, $\Gamma_3 = 0.2$, $\lambda_3 = 0.5$, $\varpi_3 = 1.0$, $\sigma_3 = 0.9$, $\delta_1 = \delta_2 = \delta_V = 1$. The numbers of NN nodes are selected as $N_V = 20$, $N_1 = 20$ and $N_2 = 20$, with their centers being evenly spaced in $[-0.5, 0.5] \times [-9.7, 9.7] \times [-4.5, 4.5] \times [0.1, 1.2]\,[-0.5, 0.5] \times [-0.5, 0.5]$ and $[-0.5, 0.5] \times [-9.7, 9.7] \times [-4.5, 4.5]$, respectively.

The reference velocity V_r of velocity subsystem simulation is achieved through a filter presented as follows.

$$\frac{V_\mathrm{r}}{V_\mathrm{c}} = \frac{0.3 \times 0.2^2}{(s + 0.3)(s^2 + 2 \times 0.7 \times 0.2s + 0.2^2)}$$

where V_c is the command signal, which climbs from 8850 ft/s to 8950 ft/s (1 ft=0.3048 m) in 20 s, and then climbs to 9150 ft/s. Moreover, the reference altitude h_r of altitude subsystem simulation is achieved through a filter presented as follows.

$$\frac{h_\mathrm{r}}{h_\mathrm{c}} = \frac{0.5 \times 0.2^2}{(s + 0.5)(s^2 + 2 \times 0.9 \times 0.2s + 0.2^2)}$$

where h_c is the command signal, which climbs from 85000 ft to 87000 ft in 40 s, and then descends to 84000 ft.

In the simulation, the initial condition is denoted in the Tab. 1.

Tab. 1 The initial values

States	Value	Units
h	85000	ft
V	8850	ft/s
γ	0	(°)
θ	0	(°)
Q	0	(°/s)

The simulation results are shown in Figs. 1–13.

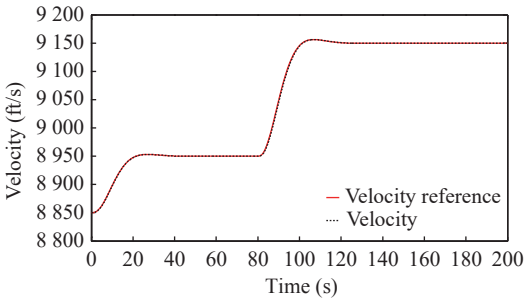

Fig. 1 Velocity tracking

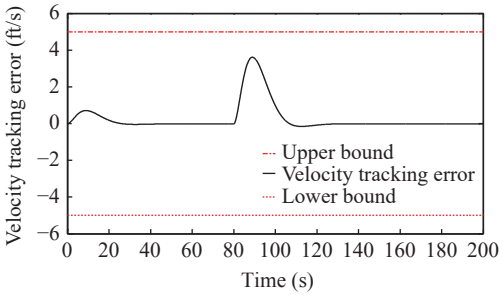

Fig. 2 Velocity tracking error

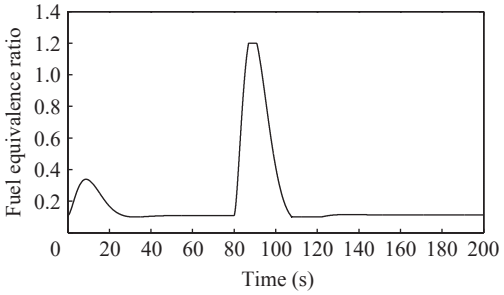

Fig. 3 Fuel equivalence ratio

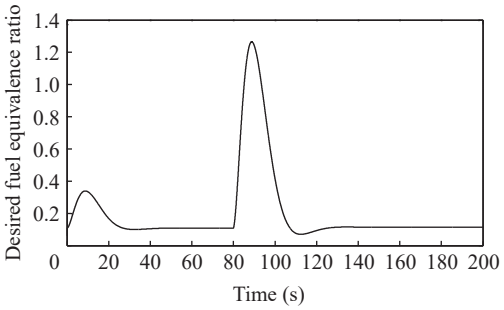

Fig. 4 Desired fuel equivalence ratio

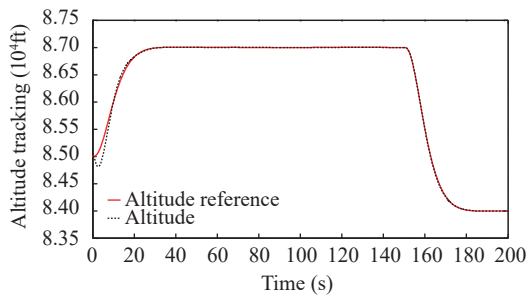

Fig. 5 Altitude tracking

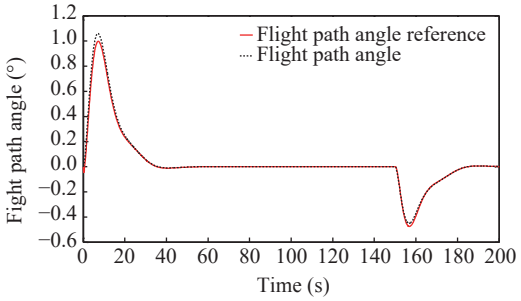

Fig. 6 Flight path angle tracking

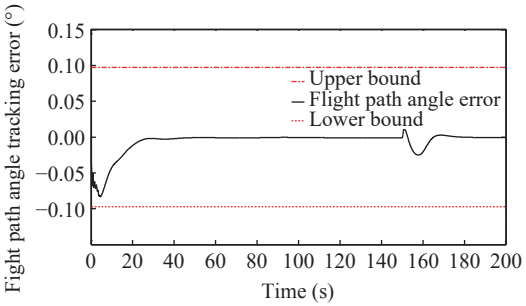

Fig. 7 Flight path angle tracking error

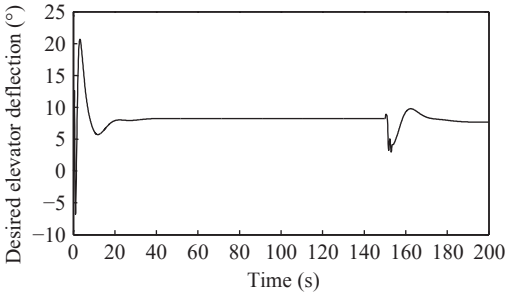

Fig. 8 Desired elevator deflection

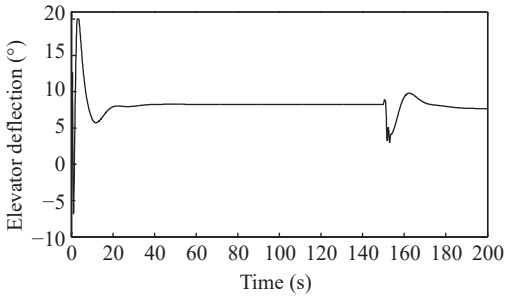

Fig. 9 Elevator deflection

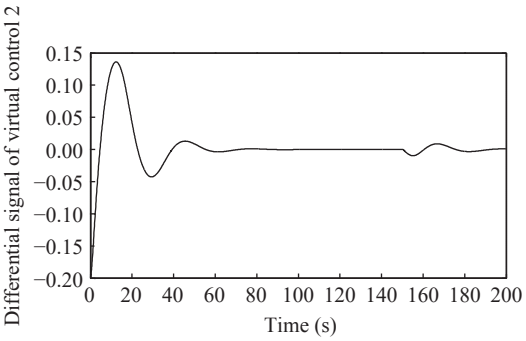

Fig. 10 Differential signal of virtual control 2

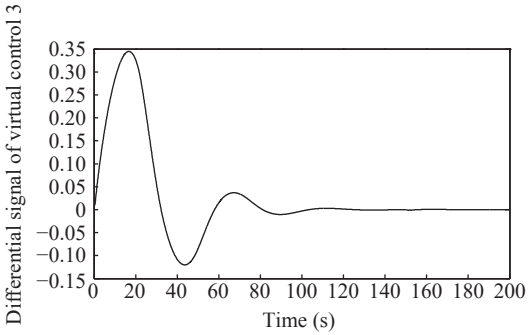

Fig. 11 Differential signal of virtual control 3

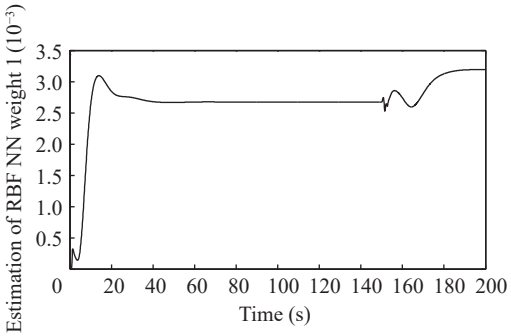

Fig. 12 Estimation of RBF NN weight 1

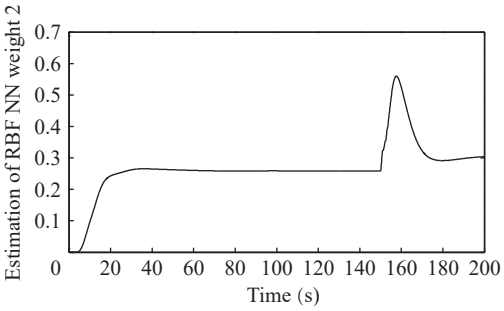

Fig. 13 Estimation of RBF NN weight 2

In Fig. 1, it is easy to see that the flight velocity of hypersonic vehicle can track the velocity reference accurately. The velocity tracking error is shown in Fig. 2, and bounded within a certain range. The upper bound is 5 ft/s, the lower bound is 5 ft/s. The Fig. 3 denotes the input signal of velocity subsystem, we can see that the fuel equivalence ratio is bounded within 0.1 to 1.2 by the saturation segment, compared with the desired fuel equivalence ratio shown in Fig. 4.

The altitude of flight vehicle can track the reference trajectory well, the altitude can climb from 85 000 ft to 87 000 ft within 30 s, and maintain a level flight at an altitude of 87 000 ft, then descends to 84 000 ft within 30 s. The desired changes design of flight altitude can simulate the maneuvering of aircraft to avoid interception. Moreover, the flight path angle tracking is shown in Fig. 6, and the flight path angle tracking error can be bounded within –0.09° to 0.09° form Fig. 7. Compared with desired elevator deflection, i.e., designed control input shown in Fig. 8, the actual elevator deflection input of altitude subsystem is bounded within –20° to 20° by the saturation segment in Fig. 9. In Fig. 9, it is easy to see that the elevator deflection exceeds the constraint, i.e., 20°, occurring from the progress of climbing from 85 000 ft to 87 000 ft. And this shows that the auxiliary system introduced in the control system design have played an important part to deal with the input saturation. The elevator deflection curve oscillation during the initial time can be seen, the reason is that the approximation errors for unknown unmodeled nonlinear dynamics by neural networks are convergent, but there is an oscillation process.

In the control system design, the tracking differentiator method is used to estimate the differential of virtual controller for overcoming the explosion of complexity raised from backstepping methods. The differential of virtual controller x_{2v} obtained from tracking differentiator is shown in Fig. 10, the signal is smooth and convergent. Likewise, the differential of virtual controller x_{3v} obtained from tracking differentiator is shown in Fig. 11. In this paper, the unknown nonlinear function is approximated by the RBF NN, and the estimation values norm of RBF NN weight can be found in Fig. 12 and Fig. 13.

6 Conclusions

In this paper, the control system design issue has been studied for hypersonic vehicle longitudinal dynamic. Because of the strong nonlinearity, coupling and dynamic model uncertainty, there are lots of difficulties for control system design. Firstly, the backstepping design method is used

in the process of controller design, the tracking differentiator is constructed for dealing with the explosion of complexity in the backstepping, the results of simulation can explain the effectiveness of tracking differentiator. Secondly, for the constraint issue of system states, the barrier Lyapunov function is applied to design the controllers of velocity subsystem and altitude subsystem respectively. Currently, this method has been applied to the design of control systems for various aircraft [29–32]. Thirdly, the RBF NN is used to approximate the unknown nonlinear functions of system dynamic, the accuracy requirements of the system dynamic model have been reduced. Furthermore, the flexible modes of hypersonic vehicle are needed to be considered in the further research work.

Conflict of Interest: The authors declare that they have no conflict of interest.

References:

[1] X. W. Bu, X. Y. Wu, and Y. X. Chen "Adaptive backstepping control of hypersonic vehicles based on nonlinear disturbance observer, " *Journal of National University of Defense Technology*, vol. 36, no. 5, pp. 44-49, 2014.

[2] B. Xu, F. Sun, C. Yang, D. Gao, and J. Ren,"Adaptive discrete-time controller design with neural network for hypersonic flight vehicle via back-stepping," *International Journal of Control*, vol. 84, no. 9, pp. 1543-1552, 2011.

[3] W. Chen and L. Jiao,"Adaptive tracking for periodically time-varying and nonlinearly parameterized systems using multilayer neural networks," *IEEE Transactions on Neural Networks*, vol. 21, no. 2, pp. 345-351, 2010.

[4] W. Chen, L. Jiao, J. Li, and R. Li,"Adaptive NN backstepping output-feedback control for stochastic nonlinear strict-feedback systems with time-varying delays," *IEEE Transactions on Systems, Man, and Cybernetics*, vol. 40, no. 3, pp. 939-950, 2010.

[5] J. Wu, J. Li, and W. Chen,"Semi-globally/globally stable adaptive NN backstepping control for uncertain MIMO systems with tracking accuracy known a priori," *Journal of the Franklin Institute*, vol. 351, no. 12, pp. 5274-5309, 2014.

[6] B. Xu, Z. Shi, C. Yang, and F. Sun,"Composite neural dynamic surface control of a class of uncertain nonlinear systems in strict-feedback form," *IEEE Transactions on Cybernetics*, vol. 14, no. 12, pp. 2626-2634, 2014.

[7] S. Swaroop, J. K. Hedrick, P. P. Yip, and J. C. Gerdes,"Dynamic surface control for a class of nonlinear systems," *IEEE Transactions on Automatic Control*, vol. 45, pp. 1893-1899, 2000.

[8] B. Xu,"Robust adaptive neural control of flexible hypersonic flight vehicle with dead-zone input nonlinearity," *Nonlinear Dynamic*, vol. 80, pp. 1509-1520, 2015.

[9] J. B. Wei, H. Y. Li, and J. Li,"Novel backstepping control for hypersonic vehicle with angle of attack constraint," *Systems Engineering and Electronics*, vol. 15, pp. 1-10, 2021.

[10] N. Nikdel, M. Badam Chizadeh, V. Azimirad, and M. A. Nazari,"Fractional-order adaptive backstepping control of robotic manipulators in the presence of model uncertainties and external disturbances," *IEEE Transactions on Industrial Electronics*, vol. 63, no. 10, pp. 6249-6256, 2016.

[11] Y. Wang and H. Wu,"Adaptive robust backstepping control for a class of uncertain dynamical systems using neural networks," *Nonlinear Dynamics*, vol. 81, no. 4, pp. 1597-1610, 2015.

[12] Y. J. Liu and S. Tong, "Barrier Lyapunov functions-based adaptive control for a class of nonlinear pure-feedback systems with full state constraints, " *Automatica*, vol. 64, no. 5, pp. 70-75, 2016.

[13] J. T. Huang, "Global adaptive neural dynamic surface control of strict-feedback systems, " *Neuro Computing*, vol. 165, pp. 403-413, 2015.

[14] B. Xu, Z. Shi, C. Yang, and S. Wang,"Neural control of hypersonic flight vehicle model via time-scale decomposition with throttle setting constraint," *Nonlinear Dynamic*, vol. 73, no. 3, pp. 1849-1861, 2013.

[15] B. Xu, D. Gao, and S. Wang,"Adaptive neural control based on hgo for hypersonic flight vehicles," *Science China-Information Sciences*, vol. 54, no. 3, pp. 511-520, 2011.

[16] X. D. Liang, "Research on attitude control of hypersonic vehicles based on online neural network regulation, " Master's thesis, Harbin Institute of Technology, 2025.

[17] M. M. Polycarpou,"Stable adaptive neural control schemes for nonlinear systems," *IEEE Transac-*

tions on Automatic Control, vol. 41, pp. 447-451, 1996.

[18] W. He and S. S. Ge,"Vibration control of a flexible string with both boundary input and output constraints," *IEEE Transactions on Control Systems Technology*, vol. 23, no. 4, pp. 1245-1254, 2015.

[19] M. Chen, S. S. Ge, and B. Ren,"Adaptive tracking control of uncertain MIMO nonlinear systems with input constraints," *Automatica*, vol. 47, no. 3, pp. 452-465, 2011.

[20] Y. Li, S. Tong, and T. Li,"Composite adaptive fuzzy output feedback control design for uncertain nonlinear strict feedback systems with input saturation," *IEEE Transactions on Cybernetics*, vol. 45, no. 10, pp. 2299-2308, 2015.

[21] Y. P. Li, F. Wang, and C. Zhou,"Prescribed performance filter backstepping control of hypersonic vehicle with full state constraints," *Acta Aeronauticaet Astronautica Sinica*, vol. 41, no. 11, pp. 623857, 2020.

[22] Z. H. Wu, J. C. Lu, Q. Zhou, and J. P. Shi,"Modified adaptive neural dynamic surface control for morphing aircraft with input and output constraints," *Nonlinear Dynamics*, vol. 87, pp. 2367-2383, 2017.

[23] K. P. Tee, S. S. Ge, and E. H. Ay,"Barrier Lyapunov functions for the control of output-constrained nonlinear systems," *Automatica*, vol. 45, no. 4, pp. 918-927, 2009.

[24] B. Ren, S. S. Ge, K. P. Tee, and T. H. Lee,"Adaptive neural control for output feedback nonlinear systems using a barrier Lyapunov function," *IEEE Transactions on Neural Networks*, vol. 21, no. 8, pp. 1339-1345, 2010.

[25] B. S. Kim and S. J. Yoo,"Adaptive control of nonlinear pure-feedback systems with output constraints: integral barrier Lyapunov functional approach," *International Journal of Control, Automation and Systems*, vol. 13, no. 1, pp. 249-256, 2014.

[26] B. S. Kim and S. J. Yoo,"Approximation-based adaptive tracking control of nonlinear pure-feedback systems with time-varying output constraints," *International Journal of Control, Automation and Systems*, vol. 13, no. 2, pp. 257-265, 2014.

[27] J. T. Parker, J. T. Parker, A. Serrani, S. Yurkovich, M. A. Bolender, and B. Doman,"Control-oriented modeling of an air-breathing hypersonic vehicle," *Journal of Guidance*, vol. 3, no. 3, pp. 856-869, 2007.

[28] Y. Lu,"Backstepping control for hypersonic flight vehicles based on tracking differentiator," *Acta Aeronautica et Astronautica Sinica*, vol. 42, no. 11, pp. 431-442, 2021.

[29] X. K. Li, H. L. Zhang, and W. H. Fan,"Finite time control of variant unmanned aerial vehicles based on time-varying obstacle Lyapunov function," *Journal of Automation*, vol. 48, no. 8, pp. 13, 2022.

[30] G. Wang and H. W. Xia,"Adaptive control of hypersonic aircraft at designated time," *Control and Decision*, vol. 38, no. 6, pp. 1602-1610, 2023.

[31] X. Wang, L. Yang, and D. W. Zhang,"Robust adaptive control of elastic hypersonic vehicles with active-passive integration," *Journal of Astronautics*, vol. 45, no. 7, pp. 1052-1064, 2024.

[32] B. Xu, Z. K. Shi, F. C. Sun, and W. He,"Barrier Lyapunov function based learning control of hypersonic flight vehicle with AOA constraint and actuator faults," *IEEE Transactions on Cybernetics*, vol. 49, no. 3, pp. 1047-1057, 2019.

Hewei Zhao received the doctor's degree in Naval Aviation Engineering College, Yantai, China, in 2017. His research interests include nonlinear control and intelligent control for aircraft.

Chengcheng Wang received the doctor's degree in Naval Aviation Engineering College, YanTai, China, in 2014. His research interests include Command Control and Fire Control.

Jing Sun is an experienced researcher in the field of the electric engineering. His current research interesrs include Circuit Analysis and signal Processing for aircraft.